J|A|C|S
ARTICLES
Published on Web 01/12/2006

Selective Formation of a Self-Assembling Homo or Hetero Cavitand Cage via Metal Coordination Based on Thermodynamic or Kinetic Control

Masamichi Yamanaka,[†] Yoshifumi Yamada,[†] Yoshihisa Sei,[‡] Kentaro Yamaguchi,[‡] and Kenji Kobayashi*[,†,§]

Contribution from the Department of Chemistry, Faculty of Science, Shizuoka University, 836 Ohya, Suruga-ku, Shizuoka 422-8529, Japan, Faculty of Pharmaceutical Sciences at Kagawa Campus, Tokushima Bunri University, Shido, Sanuki, Kagawa 769-2193, Japan, and PRESTO, JST, 4-1-8 Honcho Kawaguchi, Saitama 332-0012, Japan

Received August 12, 2005; Revised Manuscript Received December 2, 2005; E-mail: skkobay@ipc.shizuoka.ac.jp

Abstract: The selective formation of a homo or hetero cavitand cage composed of two molecules of tetra-(4-pyridyl)-cavitand (**1**), tetrakis(4-cyanophenyl)-cavitand (**2**), or tetrakis(4-pyridylethynyl)-cavitand (**3**), and four molecules of Pd(dppp)$(OTf)_2$ (**4**) or Pt(dppp)$(OTf)_2$ (**5**) has been studied. A 1:1:4 mixture of **1** with more steric restriction, **2** with less coordination ability, and **4** or **5** specifically self-assembled into a hetero cavitand cage **6** or **7**, respectively. In contrast, a 1:1:4 mixture of **2**, **3**, and **4** in $CDCl_3$ at room temperature assembled into the most labile homo cyanophenyl cavitand cage **8** and the most stable homo pyridylethynyl cavitand cage **9** in a 1:1 ratio. Upon heating at 50 °C, the thermodynamic equilibrium was shifted to a 1:1:1 mixture of **8**, **9**, and a hetero cavitand cage **10**. When 1 equiv of **3** was added to **8** at room temperature, **8**, **9**, and **10** were formed initially in a 1:1:3 ratio and finally shifted to a 1:1:1 ratio. In the Pt-system, upon addition of 1 equiv of **3** to homo cyanophenyl cavitand cage **11** in $CDCl_3$ at room temperature, the ratio of hetero to homo cavitand cage (**13**/**12**) initially attained was 8.7 and remained above 5.6 at room temperature. Upon heating at 50 °C, **13** was finally converted to **11** and **12**. Thus, the selectivity for the self-assembly of the homo or hetero cavitand cage is controlled by the balance between kinetic and thermodynamic stabilities of cages based on a combination of factors such as coordination ability and steric demand of the cavitands.

Introduction

Self-assembly of preorganized unit molecules with a concave surface provides supramolecular capsules or cages possessing an isolated nanospace.[1] Encapsulated guest molecules in these nanospaces often show different behavior from bulk phases. For example, stabilization of labile chemical species,[2] acceleration of chemical reactions,[3] and emergence of novel isomerisms[4] have been reported. Symmetrical capsules or cages have been generally adopted in these studies because of their synthetic and analytical simplicities. Some nonsymmetrical capsules or cages have been reported, mainly based on the concept of complementary ionic interaction or hydrogen bonding.[5] The nonsymmetrical nanospace provided by these assemblies has potential for novel molecular recognition events. Recently, we have reported orientational isomerism of a nonsymmetrical guest encapsulated in a hydrogen-bonded hetero dimeric capsule.[6]

[†] Shizuoka University.
[‡] Tokushima Bunri University.
[§] PRESTO.

(1) (a) MacGillivray, L. R.; Atwood, J. L. *Angew. Chem., Int. Ed.* **1999**, *38*, 1018−1033. (b) Caulder, D. L.; Raymond, K. N. *Acc. Chem. Res.* **1999**, *32*, 975−982. (c) Prins, L. J.; Reinhoudt, D. N.; Timmerman, P. *Angew. Chem., Int. Ed.* **2001**, *40*, 2382−2426. (d) Rudkevich, D. M. *Bull. Chem. Soc. Jpn.* **2002**, *75*, 393−413. (e) Hof, F.; Craig, S. L.; Nuckolls, C.; Rebek, J., Jr. *Angew. Chem., Int. Ed.* **2002**, *41*, 1488−1508. (f) Seidel, S. R.; Stang, P. J. *Acc. Chem. Res.* **2002**, *35*, 972−983. (g) Rebek, J., Jr. *Angew. Chem., Int. Ed.* **2005**, *44*, 2068−2078. (h) Fujita, M.; Tominaga, M.; Hori, A.; Therrien, B. *Acc. Chem. Res.* **2005**, *38*, 369−378.

(2) (a) Körner, S. K.; Tucci, F. C.; Rudkevich, D. M.; Heinz, T.; Rebek, J., Jr. *Chem.-Eur. J.* **2000**, *6*, 187−195. (b) Yoshizawa, M.; Kusukawa, T.; Fujita, M.; Yamaguchi, K. *J. Am. Chem. Soc.* **2000**, *122*, 6311−6312. (c) Ziegler, M.; Brumaghim, J. L.; Raymond, K. N. *Angew. Chem., Int. Ed.* **2000**, *39*, 4119−4121. (d) Yoshizawa, M.; Kusukawa, T.; Fujita, M.; Sakamoto, S.; Yamaguchi, K. *J. Am. Chem. Soc.* **2001**, *123*, 10454−10459.

(3) (a) Kang, J.; Rebek, J., Jr. *Nature* **1997**, *385*, 50−52. (b) Kang, J.; Hilmersson, G.; Santamaría, J.; Rebek, J., Jr. *J. Am. Chem. Soc.* **1998**, *120*, 3650−3656. (c) Yoshizawa, M.; Takeyama, Y.; Kusukawa, T.; Fujita, M. *Angew. Chem., Int. Ed.* **2002**, *41*, 1347−1349. (d) Yoshizawa, M.; Takeyama, Y.; Okano, T.; Fujita, M. *J. Am. Chem. Soc.* **2003**, *125*, 3243−3247. (e) Fiedler, D.; Bergman, R. G.; Raymond, K. N. *Angew. Chem., Int. Ed.* **2004**, *43*, 6748−6751.

(4) (a) Shivanyuk, A.; Rebek, J., Jr. *J. Am. Chem. Soc.* **2002**, *124*, 12074−12075. (b) Shivanyuk, A.; Rebek, J., Jr. *Angew. Chem., Int. Ed.* **2003**, *42*, 684−686. (c) Scarso, A.; Shivanyuk, A.; Rebek, J., Jr. *J. Am. Chem. Soc.* **2003**, *125*, 13981−13983. (d) Yamanaka, M.; Shivanyuk, A.; Rebek, J., Jr. *Proc. Natl. Acad. Sci. U.S.A.* **2004**, *101*, 2669−2672. (e) Yamanaka, M.; Rebek, J., Jr. *Chem. Commun.* **2004**, 1690−1691.

(5) (a) Koh, K.; Araki, K.; Shinkai, S. *Tetrahedron Lett.* **1994**, *44*, 8255−8258. (b) Lee, S. B.; Hong, J.-I. *Tetrahedron Lett.* **1996**, *37*, 8501−8504. (c) Hamelin B.; Jullien, L.; Derouet, C.; Herevé du Penhoat, C.; Berthault, P. *J. Am. Chem. Soc.* **1998**, *120*, 8438−8447. (d) Grawe, T.; Schrader, T.; Gurrath, M.; Kraft, A.; Osterod, F. *Org. Lett.* **2000**, *2*, 29−32. (e) Fiammengo, R.; Timmerman, P.; de Jong, F.; Reinhoudt, D. N. *Chem. Commun.* **2000**, 2313−2314. (f) Fiammengo, R.; Timmerman, P.; Huskens, J.; Versluis, K.; Heck, A. J. R.; Reinhoudt, D. N. *Tetrahedron* **2002**, *58*, 757−764. (g) Corbellini, F.; Fiammengo, R.; Timmerman, P.; Crego-Calame, M.; Versluis, K.; Heck, A. J. R.; Luyten, I.; Reinhoudt, D. N. *J. Am. Chem. Soc.* **2002**, *124*, 6569−6575. (h) Corbellini, F.; Costanzo, L. D.; Crego-Calame, M.; Geremia, S.; Reinhoudt, D. N. *J. Am. Chem. Soc.* **2003**, *125*, 9946−9947. (i) Corbellini, F.; Knegtel, R. M. A.; Grootenhuis, P. D. J.; Crego-Calame, M.; Reinhoudt, D. N. *Chem.-Eur. J.* **2005**, *11*, 298−307.

However, metal coordination hetero assemblies have been little reported because of the difficulty in controlling the simultaneous coordination of two kinds of ligands with different coordination ability as donors on a metal as an acceptor. Metal coordination hetero assemblies have so far been achieved based on the steric hindrance of ligands to prevent homo assembly and/or based on the inducement of a suitable guest.[7] Metal coordination hetero cavitand cages are particularly rare as compared to the corresponding homo cavitand cages.[8] Reinhoudt, Dalcanale, and coworkers reported the formation of metal coordination hetero cavitand cages on a gold surface by using two cavitands with different side chains of alkylthioether and alkyl groups at the lower rim, but with the same pyridyl or cyano ligands at the upper rim.[9] Dynamic assembly is another interesting topic, with a view to mimicking biological processes, as well as a dynamic combinatorial library of assemblies.[10] Here, we report the selective self-assembly of a homo or hetero cavitand cage that can be controlled by the balance between kinetic and thermodynamic stabilities of cages based on a combination of factors such as coordination ability and steric demand of the cavitands.[11,12]

Results and Discussion

Synthesis of Deep Cavitands and Self-Assembly of Pd-Based Hetero Cavitand Cage 6.[11] Bowl-shaped deep cavitands

Chart 1

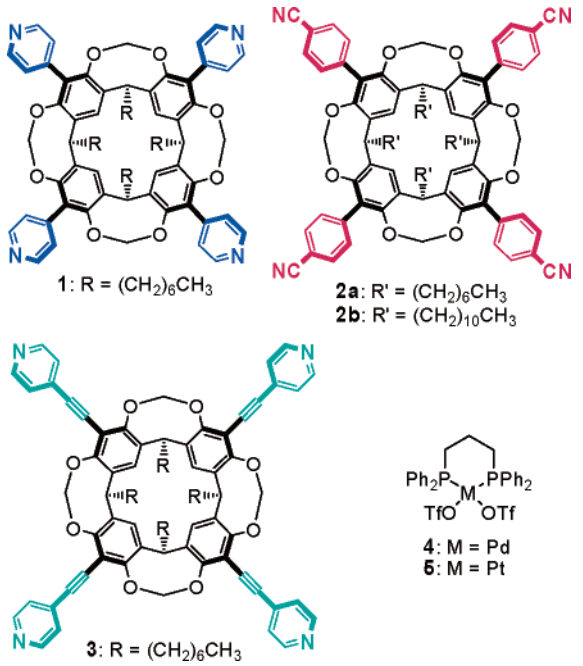

Scheme 1

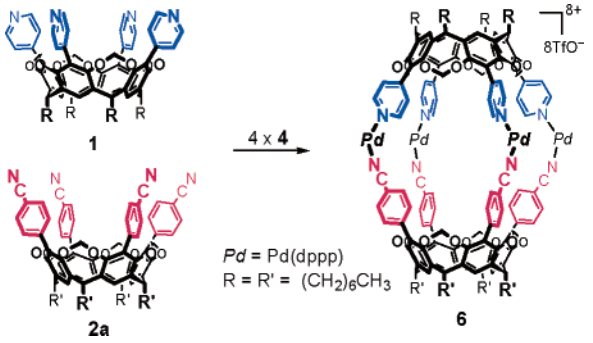

1−**3** (Chart 1) were prepared by using tetraiodocavitand as a starting material.[8m,13] Tetra(4-pyridyl)-cavitand (**1**) and tetrakis-(4-cyanophenyl)-cavitand (**2**) were synthesized by the Suzuki−Miyaura cross-coupling reaction of tetraiodocavitand with 4-pyridylboronic acid pinacol ester or 4-(cyanophenyl)boronic acid pinacol ester, respectively, in the presence of $PdCl_2(PPh_3)_2$ and $AsPh_3$.[8m,13] The Sonogashira cross-coupling reaction of tetraiodocavitand with 4-ethynylpyridine was applied to the synthesis of tetrakis(4-pyridylethynyl)-cavitand (**3**).

A 1:1:4 mixture of pyridyl cavitand **1**, cyanophenyl cavitand **2a**, and square-planar Pd(dppp)$(OTf)_2$ (**4**) in $CDCl_3$ at room temperature instantaneously and specifically self-assembled into the hetero cavitand cage $\{\mathbf{1}\cdot\mathbf{2a}\cdot[Pd(dppp)]_4\}^{8+}\cdot(TfO^-)_8$ (**6**), as shown in Scheme 1,[11] wherein **1** and **2a** as hemispheres coordinate to four molecules of **4** at the equatorial region. The

(6) (a) Kobayashi, K.; Ishii, K.; Sakamoto, S.; Shirasaka, T.; Yamaguchi, K. *J. Am. Chem. Soc*. **2003**, *125*, 10615−10624. (b) Kobayashi, K.; Ishii, K.; Yamanaka, M. *Chem.-Eur. J*. **2005**, *11*, 4725−4734.
(7) (a) Baxter, P.; Lehn, J.-M.; DeCian, A.; Fischer, J. *Angew. Chem., Int. Ed. Engl*. **1993**, *32*, 69−72. (b) Fujita, M.; Aoyagi, M.; Ibukuro, F.; Ogura, K.; Yamaguchi, K. *J. Am. Chem. Soc*. **1998**, *120*, 611−612. (c) Baxter, P. N. W.; Lehn, J.-M.; Baum, G.; Fenske, D. *Chem.-Eur. J*. **1999**, *5*, 102−112. (d) Baxter, P. N. W.; Lehn, J.-M.; Kneisel, B. O.; Baum, G.; Fenske, D. *Chem.-Eur. J*. **1999**, *5*, 113−120. (e) Garcia, A. M.; Bassani, D. M.; Lehn, J.-M.; Baum, G.; Fenske, D. *Chem.-Eur. J*. **1999**, *5*, 1234−1238. (f) Fujita, M.; Fujita, N.; Ogura, K.; Yamaguchi, K. *Nature* **1999**, *400*, 52−55. (g) Hiraoka, S.; Kubota, Y.; Fujita, M. *Chem. Commun*. **2000**, 1509−1510. (h) Sun, S.-S.; Lees, A. J. *Chem. Commun*. **2001**, 103−104. (i) Kumazawa, K.; Biradha, K.; Kusukawa, T.; Okano, T.; Fujita, M. *Angew. Chem., Int. Ed*. **2003**, *42*, 3909−3913. (j) Tominaga, M.; Kusukawa, T.; Sakamoto, S.; Yamaguchi, K.; Fujita, M. *Chem. Lett*. **2004**, 794−795. (k) Dinolfo, P. H.; Williams, M. E.; Stern, C. L.; Hupp, J. T. *J. Am. Chem. Soc*. **2004**, *126*, 12989−13001. (l) Barboiu, M.; Prodi, L.; Montalti, M.; Zaccheroni, N.; Kyritsakas, N.; Lehn, J.-M. *Chem.-Eur. J*. **2004**, *10*, 2953−2959. (m) Yoshizawa, M.; Nakagawa, J.; Kumazawa, K.; Nagano, M.; Kawano, M.; Ozeki, T.; Fujita, M. *Angew. Chem., Int. Ed*. **2005**, *44*, 1810−1813.
(8) (a) Jacopozzi, P.; Dalcanale, E. *Angew. Chem., Int. Ed. Engl*. **1997**, *36*, 613−615. (b) Fox, O. D.; Dalley, N. K.; Harrison, R. G. *J. Am. Chem. Soc*. **1998**, *120*, 7111−7112. (c) Fox, O. D.; Drew, M. G. B.; Beer, P. D. *Angew. Chem., Int. Ed*. **2000**, *39*, 136−140. (d) Fox, O. D.; Drew, M. G. B.; Wilkinson, E. J. S.; Beer, P. D. *Chem. Commun*. **2000**, 391−392. (e) Lim, C. W.; Hong, J.-I. *Tetrahedron Lett*. **2000**, *41*, 3113−3117. (f) Cuminetti, N.; Ebbing, M. H. K.; Prados, P.; de Mendoza, J.; Dalcanale, E. *Tetrahedron Lett*. **2001**, *42*, 527−530. (g) Park, S. J.; Hong, J.-I. *Chem. Commun*. **2001**, 1554−1555. (h) Fochi, F.; Jacopozzi, P.; Wegelius, E.; Rissanen, K.; Cozzini, P.; Marastoni, E.; Fisicaro, E.; Manini, P.; Fokkens, R.; Dalcanale, E. *J. Am. Chem. Soc*. **2001**, *123*, 7539−7552. (i) Pirondini, L.; Bertolini, F.; Cantadori, B.; Ugozzoli, F.; Massera, C.; Dalcanale, E. *Proc. Natl. Acad. Sci. U.S.A*. **2002**, *99*, 4911−4915. (j) Pinalli, R.; Cristini, V.; Sottili, V.; Geremia, S.; Campagnolo, M.; Caneschi, A.; Dalcanale, E. *J. Am. Chem. Soc*. **2004**, *126*, 6516−6517. (k) Park, S. J.; Shin, D. M.; Sakamoto, S.; Yamaguchi, K.; Chung, Y. K.; Lah, M. S.; Hong, J.-I. *Chem.-Eur. J*. **2005**, *11*, 235−241. (l) Zuccaccia, D.; Pirondini, L.; Pinalli, R.; Dalcanale, E.; Macchioni, A. *J. Am. Chem. Soc*. **2005**, *127*, 7025−7032. (m) Haino, T.; Kobayashi, M.; Chikaraishi, M.; Fukazawa, Y. *Chem. Commun*. **2005**, 2321−2323.
(9) (a) Levi, S. A.; Guatteri, P.; van Veggel, F. C. J. M.; Vancso, G. J.; Dalcanale, E.; Reinhoudt, D. N. *Angew. Chem., Int. Ed*. **2001**, *40*, 1892−1896. (b) Menozzi, E.; Pinalli, R.; Speets, E. A.; Ravoo, B. J.; Dalcanale, E.; Reinhoudt, D. N. *Chem.-Eur. J*. **2004**, *10*, 2199−2206.
(10) For example: (a) Hof, F.; Nuckolls, C.; Rebek, J., Jr. *J. Am. Chem. Soc*. **2000**, *122*, 4251−4252. (b) Kubota, Y.; Sakamoto, S.; Yamaguchi, K.; Fujita, M. *Proc. Natl. Acad. Sci. U.S.A*. **2002**, *99*, 4854−4856.
(11) For a preliminary report on the Pd-based hetero cavitand cage **6**, see: Kobayashi, K.; Yamada, Y.; Yamanaka, M.; Sei, Y.; Yamaguchi, K. *J. Am. Chem. Soc*. **2004**, *126*, 13896−13897.
(12) For kinetic control in metal−ligand self-assembly, see: (a) Hasenknopf, B.; Lehn, J.-M.; Boumediene, N.; Leize, E.; Dorsselaer, A. V. *Angew. Chem., Int. Ed*. **1998**, *37*, 3265−3268. (b) Paraschiv, V.; Crego-Calama, M.; Ishi-i, T.; Padberg, C. J.; Timmerman, P.; Reinhoudt, D. N. *J. Am. Chem. Soc*. **2002**, *124*, 7638−7639. (c) Tashiro, S.; Tominaga, M.; Kusukawa, T.; Kawano, M.; Sakamoto, S.; Yamaguchi, K.; Fujita, M. *Angew. Chem., Int. Ed*. **2003**, *42*, 3267−3270. (d) Badjiæ, J. D.; Cantrill, S. J.; Stoddart, J. F. *J. Am. Chem. Soc*. **2004**, *126*, 2288−2289. (e) Hori, A.; Yamashita, K.; Fujita, M. *Angew. Chem., Int. Ed*. **2004**, *43*, 5016−5019.
(13) Sebo, L.; Diederich, F.; Gramlich, V. *Helv. Chim. Acta* **2000**, *83*, 93−113.

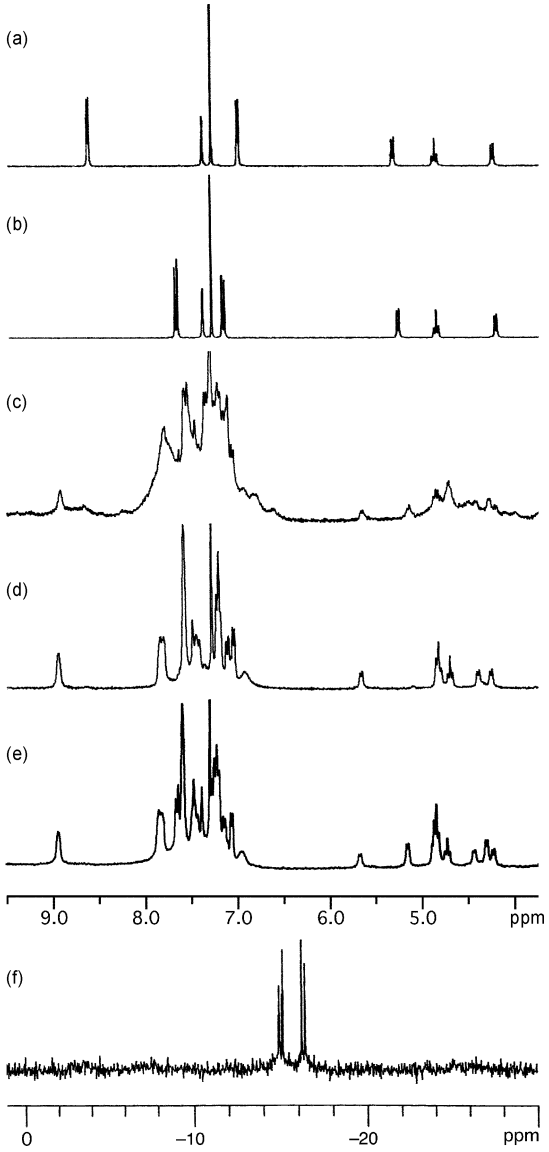

Figure 1. ^{1}H NMR spectra (300 MHz, $CDCl_3$, 296 K) of (a) **1**, (b) **2a**, (c) [**1**] = [**2a**] = 1 mM and [**5**] = 4 mM immediately after the mixing, (d) a mixture of [**1**] = [**2a**] = 1 mM and [**5**] = 4 mM after the heating at 50 °C for 13 h (hetero cavitand cage **7**), and (e) a mixture of [**1**] = 1 mM, [**2a**] = 2 mM, and [**5**] = 4 mM after the heating at 50 °C for 13 h (**7** and free **2a**); (f) ^{31}P NMR spectrum (162 MHz, $CDCl_3$, 296 K) of a mixture of [**1**] = [**2a**] = 1 mM and [**5**] = 4 mM after the heating at 50 °C for 13 h (**7**).

structure of **6** was determined by ^{1}H and ^{31}P NMR spectroscopies and cold-spray ionization mass spectrometry (CSI-MS).[14] This specific self-assembly would arise from a combination of factors such as coordination ability and steric demand of the cavitands. The pyridyl group of **1** is more sterically hindered than the cyanophenyl group of **2a** toward the dppp on the Pd, whereas the inherent coordination ability of the former is greater than that of the latter. The rotation of pyridyl and cyanophenyl groups on the cavitand scaffold is highly restricted because the ligand moiety is placed between the two oxygen atoms on the cavitand scaffold. Thus, simultaneous cis-coordination of the pyridyl group of two molecules of **1** to Pd(dppp) did not form a homo cavitand cage $\{(\mathbf{1})_2\cdot[Pd(dppp)]_4\}^{8+}\cdot(TfO^-)_8$, but gave complicated aggregates. Upon addition of 1 equiv of **2a**, aggregates were converted to **6**. For these reasons,

(14) Yamaguchi, K. *J. Mass Spectrom.* **2003**, *38*, 473−490.

Scheme 2

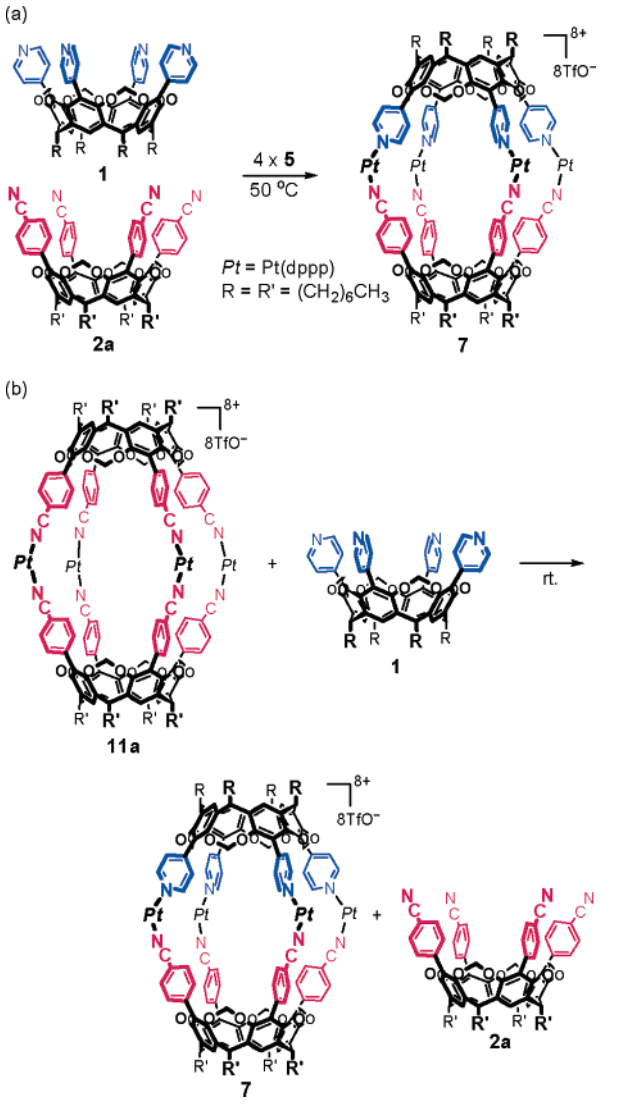

the hetero cavitand cage **6** is specifically formed as the most thermodynamically stable species.

Self-Assembly of Pt-Based Hetero Cavitand Cage 7. In contrast to the Pd-based hetero cavitand cage **6**, the ^{1}H NMR spectrum of a 1:1:4 mixture of **1**, **2a**, and $Pt(dppp)(OTf)_2$ (**5**) in $CDCl_3$ at room temperature showed complicated and broad signals, although a hetero cavitand cage may be contained (Figure 1c). It is well known that the Pt−pyridine bond is kinetically more stable than the Pd−pyridine bond.[15] Thus, in this mixture, pyridyl cavitand **1**, with stronger coordination ability than **2a**, and $Pt(dppp)(OTf)_2$ (**5**) would preferentially assemble into unidentified aggregates based on kinetic control. However, after this mixture was heated at 50 °C for 13 h, the ^{1}H NMR spectrum showed the complete change of the complicated aggregates to a single highly symmetrical species (C_{4v} symmetry), indicating the hetero cavitand cage $\{\mathbf{1}\cdot\mathbf{2a}\cdot[Pt(dppp)]_4\}^{8+}\cdot(TfO^-)_8$ (**7**), as shown in Scheme 2a and Figure 1d. In the **1** unit of **7**, the $\Delta\delta$ values ($\Delta\delta = \delta_{cage} - \delta_{freeligand}$) of the inner and outer protons of the methylene-bridge and the pyridyl α- and *β*-protons were +0.17, +0.46, +0.31, and +0.05

(15) Fujita, M.; Ibukuro, F.; Yamaguchi, K.; Ogura, K. *J. Am. Chem. Soc.* **1995**, *117*, 4175−4176.

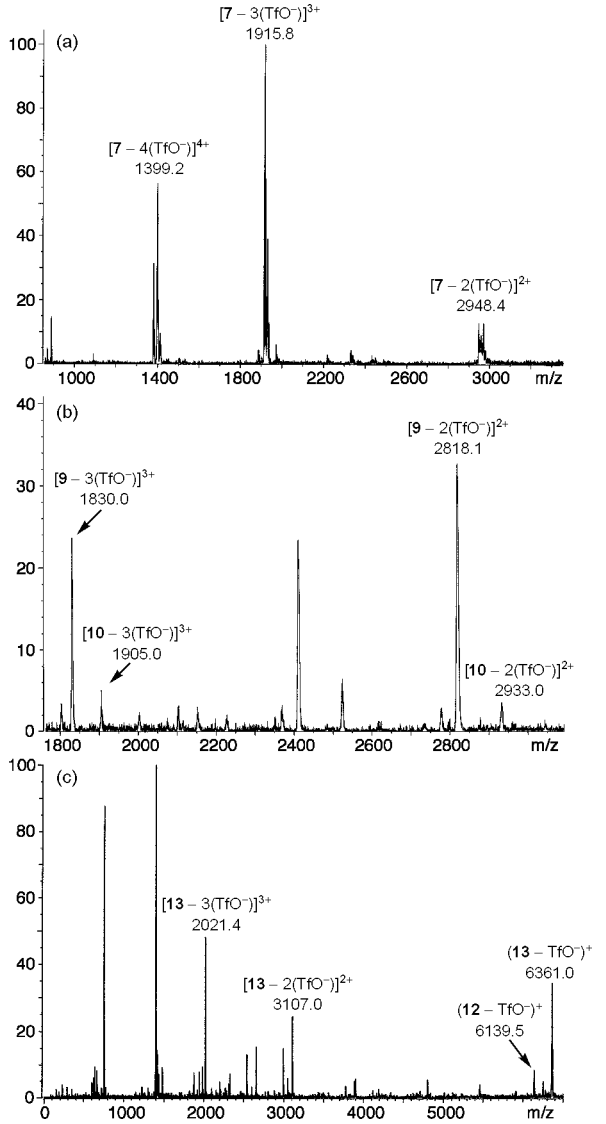

Figure 2. CSI-MS spectra of (a) a mixture of **1**, **2a**, and **5** (hetero cavitand cage **7**), (b) a mixture of **3** and **8** (cavitand cages **8**, **9**, and **10**), and (c) a mixture of **3** and **11b** (cavitand cages **11b**, **12**, and **13**) in $CHCl_3$ at the spray temperature of −20 °C.

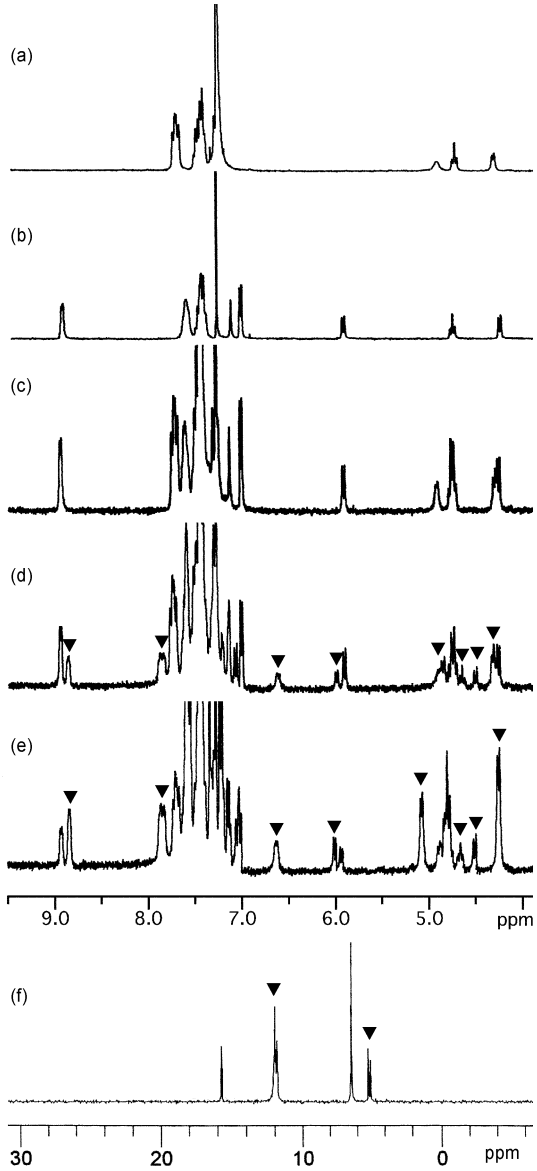

Figure 3. ^{1}H NMR spectra (300 MHz, $CDCl_3$, 296 K) of (a) [**2b**] = 2 mM and [**4**] = 4 mM (homo cavitand cage **8**), (b) [**3**] = 2 mM and [**4**] = 4 mM (homo cavitand cage **9**), (c) [**2b**] = [**3**] = 1 mM and [**4**] = 4 mM immediately after the mixing (**8** and **9**), (d) [**2b**] = [**3**] = 1 mM and [**4**] = 4 mM after the heating at 50 °C for 6 h (**8**, **9**, and hetero cavitand cage **10**), and (e) [**3**] = [**8**] = 1 mM (**10**/**9** = 3.0); (f) ^{31}P NMR spectrum (162 MHz, $CDCl_3$, 296 K) of [**3**] = [**8**] = 1 mM. The typical signals of the hetero cavitand cage **10** are marked with ▼.

ppm, respectively, and in the **2a** unit of **7**, the $\Delta\delta$ values of the inner and outer protons of the methylene-bridge and the α- and β-protons of the *p*-cyanophenyl group were +0.07, −0.42, ca. −0.2 (overlap), and −0.04 ppm, respectively (Figure 1a,b vs 1d). The ^{31}P NMR spectrum of **7** showed two doublet peaks at −16.31 and −15.02 ppm with the same coupling constant of $^2J_{P-P}$ = 31.9 Hz due to the dppp desymmetrized by the hetero cavitand cage formation (Figure 1f). Further evidence for the formation of **7** was given by the CSI-MS, wherein the molecular ion peaks of **7** were observed at *m*/*z* 2948.4 [**7** − 2(TfO$^-$)]$^{2+}$ (calcd 2947.8), 1915.8 [**7** − 3(TfO$^-$)]$^{3+}$ (1915.5), and 1399.2 [**7** − 4(TfO$^-$)]$^{4+}$ (1399.2), as shown in Figure 2a.

The hetero cavitand cage **7** once formed was thermodynamically stable and retained the structure without further transformation. Exchange between the **2a** unit of **6** and free **2a** was fast on the NMR time scale,[11] whereas exchange between the **2a** unit of **7** and free **2a** was slow on the NMR time scale (Figure 1e). The Pt−NCPh bond is thermodynamically, as well as kinetically, less stable than the Pt−pyridine bond. In fact, the homo cyanophenyl-cavitand cage {(**2a**)$_2$·[Pt(dppp)]$_4$}$^{8+}$·(TfO$^-$)$_8$ (**11a**) (vide infra) in $CDCl_3$ at room temperature gradually underwent ligand exchange with 1 equiv of **1** to give a 1:1 mixture of **7** and free **2a** after 24 h (Scheme 2b). The ^{1}H NMR spectrum was identical to Figure 1e.

Self-Assembly of Cyanophenyl Cavitand 2b, Pyridylethynyl Cavitand 3, and Pd(dppp)(OTf)$_2$ (4). Pyridylethynyl cavitand **3** has an ethynyl moiety between the cavitand scaffold and the pyridine ring. The pyridyl group of **3** is free from steric hindrance that arises from the restriction of free rotation of the pyridine ring in pyridyl cavitand **1**. Consequently, the ^{1}H NMR spectrum of a 2:4 mixture of **3** and Pd(dppp)(OTf)$_2$ (**4**) showed the quantitative formation of homo pyridylethynyl cavitand cage {(**3**)$_2$·[Pd(dppp)]$_4$}$^{8+}$·(TfO$^-$)$_8$ (**9**), as shown in Figure 3b. In contrast to a 1:1:4 mixture of **1**, **2a**, and **4** to form the hetero

Scheme 3

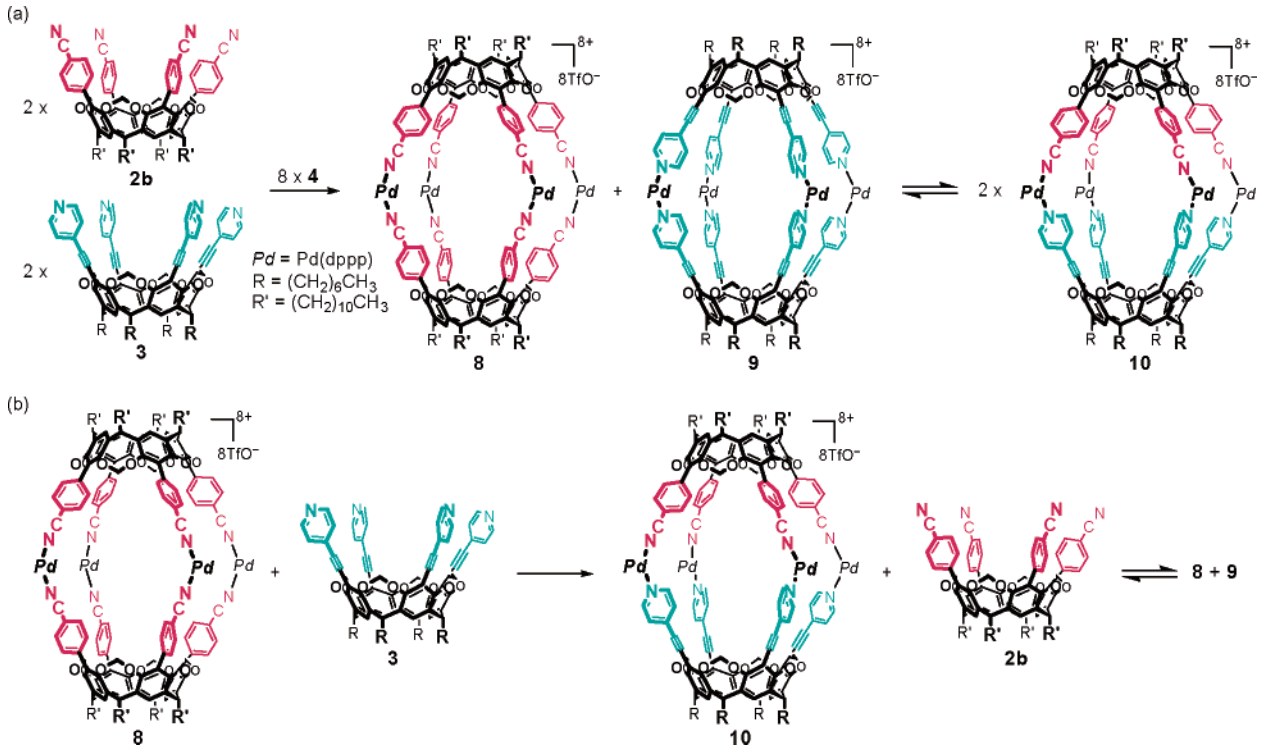

cavitand cage **6**, a 1:1:4 mixture of cyanophenyl cavitand **2b** (1 mM), **3**, and **4** in $CDCl_3$ instantaneously produced the most labile homo cyanophenyl cavitand cage $\{(\mathbf{2b})_2\cdot[Pd(dppp)]_4\}^{8+}\cdot(TfO^-)_8$ (**8**) and the most stable **9** in a 1:1 ratio (Figure 3c).[11] The coordination ability of pyridylethynyl cavitand **3** is much higher than that of cyanophenyl cavitand **2**. Therefore, homo pyridylethynyl cavitand cage **9** forms prior to homo cyanophenyl cavitand cage **8**. At the initial state of cavitand cage formation, **9** formation based on kinetic control is the driving force of the self-assembly and **8** is the byproduct. However, new signals appeared from the 1:1:4 solution of **2b** (1 mM), **3**, and **4** after heating at 50 °C, as marked with a ▼ in Figure 3d, in addition to **8** and **9**. We found that these new signals result from the hetero cavitand cage $\{\mathbf{2b}\cdot\mathbf{3}\cdot[Pd(dppp)]_4\}^{8+}\cdot(TfO^-)_8$ (**10**) (Scheme 3a). In the **3** unit of **10**, the $\Delta\delta$ values ($\Delta\delta = \delta_{cage} - \delta_{freeligand}$) of the inner and outer protons of the methylene-bridge and the pyridyl α- and *β*-protons were −0.08, −0.03, +0.24, and −0.11 ppm, respectively, and in the **2b** unit of **10**, the $\Delta\delta$ values of the inner and outer protons of the methylene-bridge and the α- and *β*-protons of the *p*-cyanophenyl group were ca. +0.55 (overlap), ca. −0.35 (overlap), −0.59, and −0.52 ppm, respectively (Figure 3a,b vs 3d). In Figure 3f, the ^{31}P NMR spectrum showed two doublet peaks at 5.18 and 11.88 ppm with the same coupling constant of $^2J_{P-P} = 27.3$ Hz in **10** due to the desymmetrization of dppp by the hetero cage formation, together with two singlet peaks of **8** (15.71 ppm) and **9** (6.47 ppm). The CSI-MS of a 1:1:4 mixture of **2b**, **3**, and **4** in $CHCl_3$ after heating at 50 °C showed molecular ion peaks of hetero cavitand cage **10** at *m*/*z* 2933.0 $[\mathbf{10} - 2(TfO^-)]^{2+}$ (calcd 2930.7) and 1905.0 $[\mathbf{10} - 3(TfO^-)]^{3+}$ (calcd 1904.2) as independent peaks from the homo cavitand cages (Figure 2b).[16]

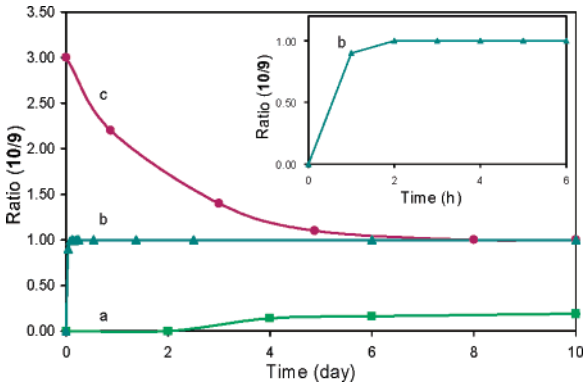

Figure 4. Ratios of hetero cavitand cage **10** to homo cavitand cage **9** as a function of time (day), monitored by ^1H NMR integration:[17] (a) [**2b**] = [**3**] = 1 mM and [**4**] = 4 mM in $CDCl_3$ at 23 °C (0 h: **10**/**9** = 0); (b) [**2b**] = [**3**] = 1 mM and [**4**] = 4 mM in $CDCl_3$ at 50 °C (0 h: **10**/**9** = 0); (c) [**3**] = [**8**] = 1 mM in $CDCl_3$ at 23 °C (0 h: **10**/**9** = 3.0).

A 1:1 mixture of homo cavitand cages **8** and **9** was converted into a mixture of **8**, **9**, and **10** (Scheme 3a and Figure 4a,b). The conversion at room temperature was slow, as shown in Figure 4a.[17] Homo cavitand cages (**10**/**9** = 0) were retained for at least 2 days. However, hetero cavitand cage **10** appeared after 4 days (**10**/**9** = 0.14). Afterward, the ratio of **10** slowly increased (24 days, **10**/**9** = 0.21; 60 days, **10**/**9** = 0.46; 134 days, **10**/**9** = 0.97). Finally, the ratio reached the thermodynamic equilibrium value of 1.0. The conversion at 50 °C proceeded more quickly, as shown in Figure 4b (1 h, **10**/**9** = 0.90; 2 h, **10**/**9** = 1.0). Afterward, the ratio of **10**/**9** = 1.0 was remained unchanged.

(16) Cavitand **2b** [R′ = $(CH_2)_{10}CH_3$] was used in place of **2a** [R′ = $(CH_2)_6CH_3$] because the formula of **2a** is identical to that of **3**. Otherwise, the molecular weight of the hetero cavitand cage is equal to that of the homo cavitand cage.

(17) We used ^1H NMR integration to determine the molar ratios of homo and hetero cavitand cages. Inner and outer protons of methylene bridges and α-protons of pyridine rings of cages were used for the integration ratios. Molar ratios based on the integration of ^{31}P NMR signals, as well as the integration of ^1H NMR signals, were calculated at the initial state. The integral ratios of homo and hetero cavitand cages from ^{31}P NMR signals were consistent with those from ^1H NMR signals.

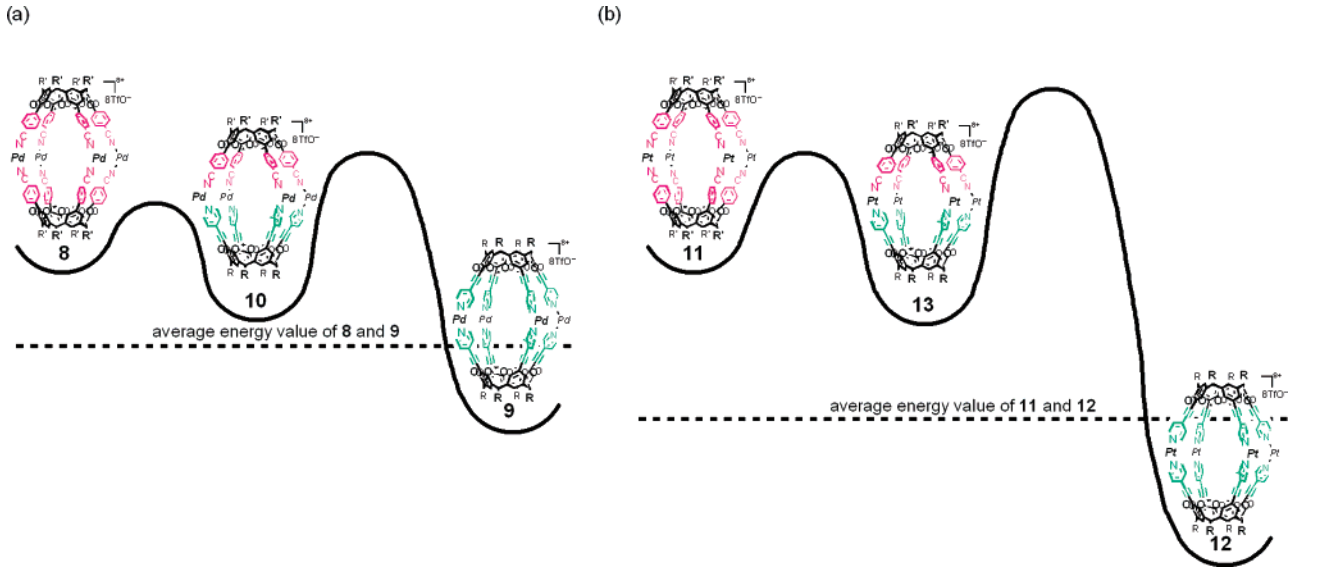

Figure 5. Schematic representation of relative energy diagrams for (a) Pd-based cavitand cages **8**, **9**, and **10**, and (b) Pt-based cavitand cages **11**, **12**, and **13**.

Hetero cavitand cage **10** is selectively formed by controlling the addition order and stoichiometry of cavitand ligands. Partial ligand exchange between the most labile homo cavitand cage **8** and **3** based on kinetic control would proceed to form a mixture enriched in hetero cavitand cage **10** prior to exchange toward homo cavitand cage **9** (Scheme 3b). Upon slow addition of 1 equiv of pyridylethynyl cavitand **3** to a solution of homo cavitand cage **8**, the ratio of **10**/**9** reached up to 3.0 at the initial stage (Figure 3e). The hetero cavitand cage enriched mixture (**10**/**9** = 3.0) was shifted to the thermodynamic equilibrium state (**10**/**9** = 1.0) after 1 week at room temperature (Figure 4c).

The 1:1:1 product ratio of **8**, **9**, and **10** at the thermodynamic equilibrium state starting from a *n*:1:4 ($n \geq 1$) of **2b**, **3**, and **4** would be explained as follows. The relative energy diagram for **8**, **9**, and **10** is shown in Figure 5a. Homo cavitand cage **9** constructed from pyridylethynyl cavitand **3** with stronger coordination ability is the most stable cage among **8**, **9**, and **10**, whereas homo cavitand cage **8** composed of cyanophenyl cavitand **2b** with weaker coordination ability is thermodynamically the most labile among them. A 1:2:4 mixture of **2b**, **3**, and **4** gave only homo cavitand cage **9**. In contrast, a 2:1:4 mixture of **2b**, **3**, and **4** produced **8**, **9**, and **10** in the 1:1:1 ratio, which is the same as the product ratio obtained from the 1:1:4 system of **2b**, **3**, and **4** described above. A 1:3:8 mixture of **2b**, **3**, and **4** produced **8**, **9**, and **10** in the 0.33:1.33:0.33 ratio at the thermodynamically equilibrium state. The thermodynamic stability of hetero cavitand cage **10** constructed from two different cavitand ligands **2b** and **3** would lie between those of the two homo cavitand cages **8** and **9**. In the 1:1:4 mixture of **2b**, **3**, and **4**, the formation of **9** is inevitably accompanied by the formation of **8** in the 1:1 ratio. Therefore, the thermodynamic equilibrium point in this system lies between the average thermodynamic stability of the two homo cavitand cages (**8** and **9**) and the thermodynamic stability of hetero cavitand cage **10** (Figure 5a). The conversion rate to reach thermodynamic equilibrium starting from homo cavitand cages **8** and **9** was much slower than that starting from the hetero cavitand cage **10** enriched system (Scheme 3a vs b and Figure 4a vs c). The difference results from the fact that formation of **10** starting from **8** and **9** requires dissociation of **3** from the thermodynamically most stable **9** (Figure 5a). The cavitand ligand exchange to produce **10** is promoted by heating the mixture at 50 °C (Figure 4b).

Self-Assembly of Cyanophenyl Cavitand 2, Pyridylethynyl Cavitand 3, and Pt(dppp)(OTf)$_2$ (5). A 2:4 mixture of cyanophenyl cavitand **2b** and Pt(dppp)(OTf)$_2$ (**5**) self-assembled into homo cavitand cage $\{(\mathbf{2b})_2 \cdot [Pt(dppp)]_4\}^{8+} \cdot (TfO^-)_8$ (**11b**) (Figure 6a).[8f] A 2:4 mixture of pyridylethynyl cavitand **3** and **5** gave homo cavitand cage $\{(\mathbf{3})_2 \cdot [Pt(dppp)]_4\}^{8+} \cdot (TfO^-)_8$ (**12**) (Figure 6b). Upon addition of 4 equiv of **5** to a 1:1 mixture of **2b** and **3** in $CDCl_3$, the ^{1}H NMR spectrum showed the formation of a 1:1:*n* ($n \geq 1$) mixture of **11b**, **12**, and hetero cavitand cage $\{\mathbf{2b} \cdot \mathbf{3} \cdot [Pt(dppp)]_4\}^{8+} \cdot (TfO^-)_8$ (**13**), marked with ▼, as shown in Figure 6c and Scheme 4a. In the **3** unit of **13**, the $\Delta\delta$ values ($\Delta\delta = \delta_{cage} - \delta_{freeligand}$) of the inner and outer protons of the methylene-bridge and the pyridyl α- and *β*-protons in $CDCl_3$ were −0.09, −0.02, +0.28, and ca. −0.1 (overlap) ppm, respectively, and in the **2b** unit of **13**, the $\Delta\delta$ values of the inner and outer protons of the methylene-bridge and the α- and *β*-protons of the *p*-cyanophenyl group in $CDCl_3$ were +0.13, −0.44, −0.59, and −0.54 ppm, respectively. The ^{31}P NMR spectrum in CD_2Cl_2 showed two doublet peaks at −17.01 and −12.37 ppm with the same coupling constant of $^2J_{P-P} = 31.9$ Hz in **13**, in addition to the peaks of homo cavitand cages **11b** (−15.14 ppm) and **12** (−15.11 ppm), as shown in Figure 6f. These results support hetero cavitand cage **13**. Further identification of **13** was obtained by CSI-MS, wherein the molecular ion peaks were observed at 6361.0 $(\mathbf{13} - TfO^-)^+$ (calcd 6365.4), 3107.0 $[\mathbf{13} - 2(TfO^-)]^{2+}$ (calcd 3108.2), and 2021.4 $[\mathbf{13} - 3(TfO^-)]^{3+}$ (calcd 2022.4) as independent peaks from the homo cavitand cages (Figure 2c).

Addition of cyanophenyl cavitand **2b** (1 equiv to **3**) to the solution of homo cavitand cage **12** and free **5**, which is prepared by mixing pyridylethynyl cavitand **3** and Pt(dppp)(OTf)$_2$ (**5**) in a 1:4 ratio, gave only homo cavitand cages **11b** and **12** in a 1:1 ratio (Figure 6d and Scheme 4b). Once homo cavitand cages **11b** and **12** are formed, they are stable even at 50 °C and remained unchanged for more than 2 months (Figure 7a).

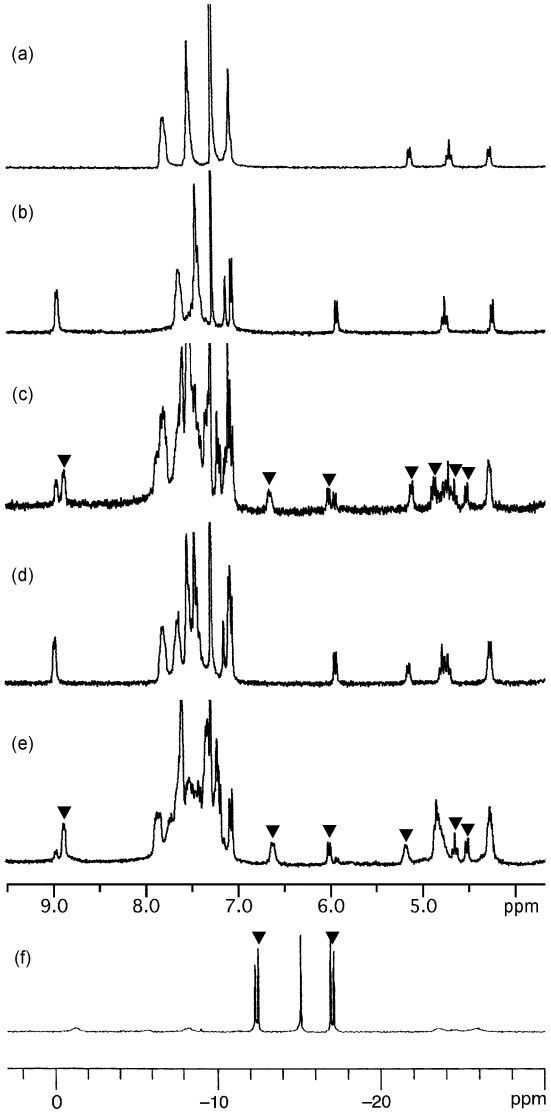

Figure 6. ^{1}H NMR spectra (300 MHz, $CDCl_3$, 296 K) of (a) [**2b**] = 2 mM and [**5**] = 4 mM (homo cavitand cage **11b**), (b) [**3**] = 2 mM and [**5**] = 4 mM (homo cavitand cage **12**), (c) [**2b**] = [**3**] = 1 mM and [**5**] = 4 mM (**2b**, **3**, and **5** were mixed at once) (**11b**, **12**, and hetero cavitand cage **13**), (d) [**2b**] = 1 mM, [**12**] = 0.5 mM, and [**5**] = 2 mM (**11b** and **12**), and (e) [**3**] = [**11b**] = 1 mM (**13**/**12** = 8.7); (f) ^{31}P NMR spectrum (162 MHz, CD_2Cl_2, 296 K) of [**3**] = [**11b**] = 2 mM. The typical signals of the hetero cavitand cage **13** are marked with ▼.

A kinetic-controlled hetero cavitand cage formation procedure, as demonstrated in the Pd-based **10** formation, was also effective for Pt-based **13** formation. Hetero cavitand cage **13** was formed selectively by adding 1 equiv of **3** to a solution of homo cavitand cage **11b**. The initial ratio of **13**/**12** reached up to 8.7 in $CDCl_3$ (Scheme 4c and Figures 6e and 7c).[17] An increase of homo cavitand cages was observed in the hetero cavitand cage enriched solution (**13**/**12** = 5.6) by heating at 50 °C (Figure 7b). The ratio of **13**/**12** became 2.0 after 12 h, and further transformation to homo cavitand cages proceeded. Finally, the hetero cavitand cage **13** was converted completely into homo cavitand cages **11b** and **12** after 30 days at 50 °C. The thermodynamic stability of **13** would be between those of **11b** and **12**, as was the case with Pd-based cavitand cages. The fact that only **11b** and **12** specifically exist at the final thermodynamic equilibrium state indicates that the average thermodynamic stability of **11b** and **12** is much greater than

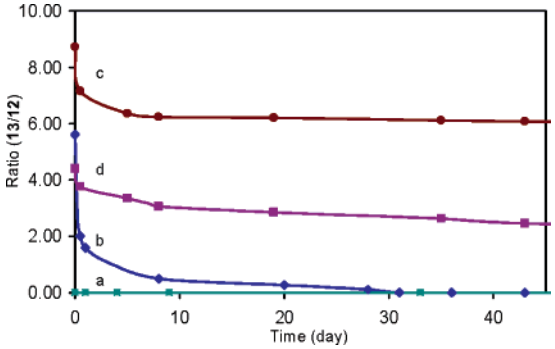

Figure 7. Ratios of hetero cavitand cage **13** to homo cavitand cage **9** as a function of time (day), monitored by ^{1}H NMR integration:[17] (a) [**2b**] = 1 mM, [**12**] = 0.5 mM and [**5**] = 2 mM in $CDCl_3$ at 50 °C (0 h: **13**/**12** = 0); (b) [**11b**] = [**3**] = 1 mM in $CDCl_3$ at 50 °C (0 h: **13**/**12** = 5.6); (c) [**11b**] = [**3**] = 1 mM in $CDCl_3$ at 23 °C (0 h: **13**/**12** = 8.7); (d) [**11b**] = [**3**] = 1 mM in acetone-d_6 at 23 °C (0 h: **13**/**12** = 4.4).

the thermodynamic stability of **13** (Figure 5b) because **12** is thermodynamically much more stable than **11b** and **13**. On the other hand, a solution enriched in hetero cavitand cage **13**, which is prepared by the method of Scheme 4c, fairly maintains the ratio at room temperature, as shown in Figure 7c (0 h, **13**/**12** = 8.7; 12 h, **13**/**12** = 7.2; 90 days, **13**/**12** = 6.0; 175 days, **13**/**12** = 5.6). Transformation to the thermodynamically stable cavitand cage was influenced by the polarity of the solvent. In acetone-d_6, a more polar solvent than $CDCl_3$, the ratio of homo cavitand cages **11b** and **12** gradually increased at room temperature, as shown in Figure 7d (0 h, **13**/**12** = 4.4; 90 days, **13**/**12** = 1.65; 175 days, **13**/**12** = 1.03).

Conclusions

We have demonstrated selective formation of self-assembling homo or hetero cavitand cages via metal coordination based on thermodynamic and kinetic control. A 1:1:4 mixture of pyridyl cavitand **1** with more steric restriction, cyanophenyl cavitand **2a** with less coordination ability, and Pd(dppp)$(OTf)_2$ (**4**) or Pt(dppp)$(OTf)_2$ (**5**) in $CDCl_3$ self-assembled into the thermodynamically stable hetero cavitand cage **6** or **7**, respectively, based on a combination of coordination ability and steric demand of the cavitand ligands. Pyridylethynyl cavitand **3** has less steric restriction than **1** and more coordination ability than **2**. A 1:1:4 mixture of **2b**, **3**, and **4** at room temperature self-assembled into kinetically as well as thermodynamically the most stable homo pyridylethynyl cavitand cage **9** and the most labile homo cyanophenyl cavitand cage **8** in the 1:1 ratio. Upon heating this mixture at 50 °C for 2 h, the thermodynamic equilibrium was shifted to a 1:1:1 mixture of **8**, **9**, and the hetero cavitand cage **10**. Upon addition of 1 equiv of **3** to **8** at room temperature, a mixture enriched in hetero cavitand cage **10** (**10**/**9** = 3.0) was obtained at the initial state. In the Pt-system, a 1:1:4 mixture of **2b**, **3**, and **5** gave a mixture of homo cyanophenyl cavitand cage **11b**, homo pyridylethynyl cavitand cage **12**, and hetero cavitand cage **13** in a 1:1:n ($n \geq 1$) ratio. Upon addition of 2 equiv of **2b** to a 1:4 mixture of **12** and **5**, two homo cavitand cages **11b** and **12** were specifically formed in the 1:1 ratio. This mixture remained unchanged upon heating at 50 °C, due to thermodynamically the most stable **12**. Selective formation of hetero cavitand cage **13** was attained by adding 1 equiv of **3** to the solution of homo cavitand cage **11b**, and the ratio of **13**/**12** reached up to 8.7 at the initial state and remained above 5.6 at

Scheme 4

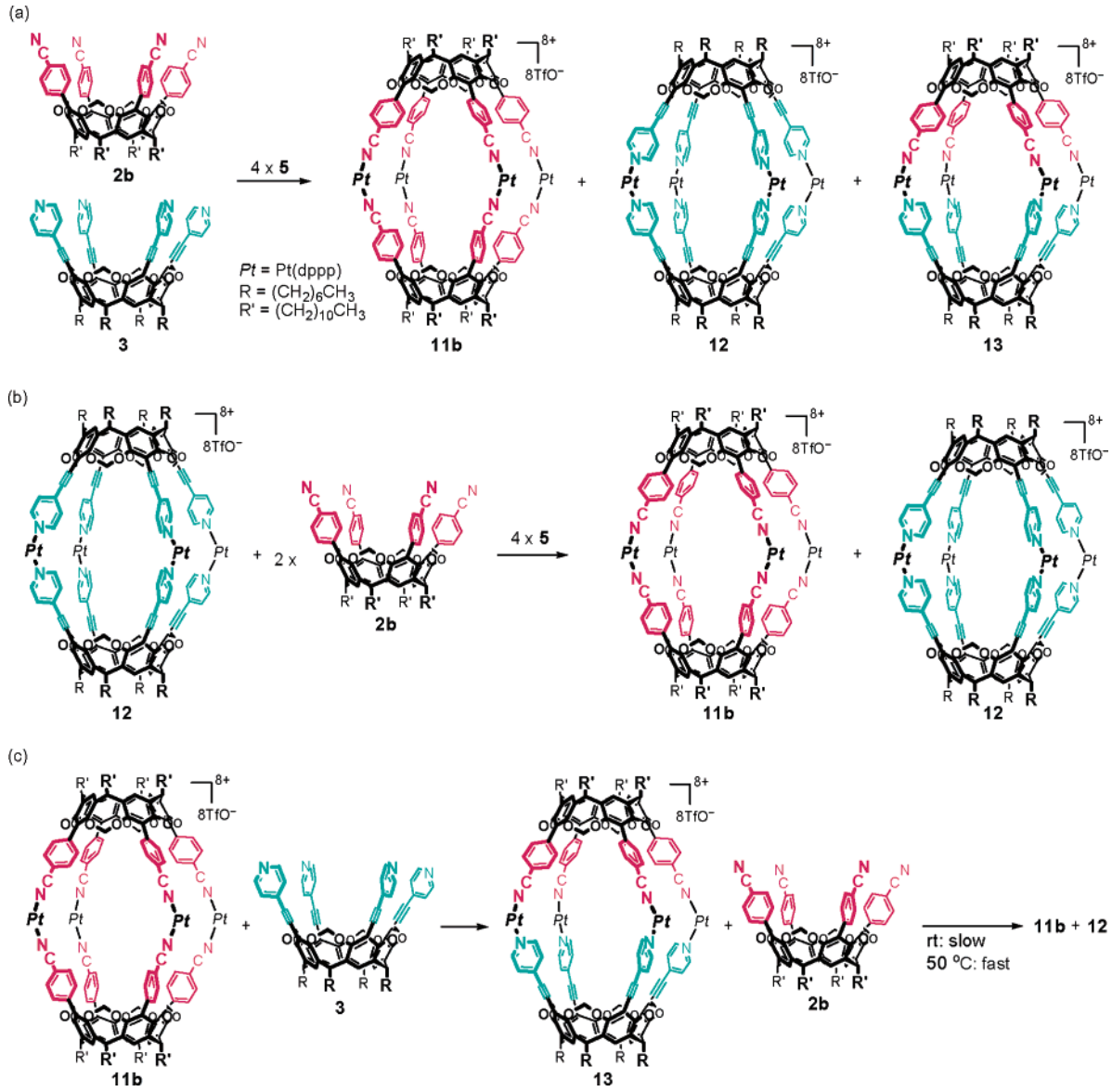

room temperature even after a half of a year, due to the kinetic stability of the Pt−ligand bond. However, upon heating at 50 °C, the ratio of **13**/**12** decreased to 2.0 after 12 h, and **13** was completely converted to **11b** and **12** after 30 days. The average thermodynamic stability of **11b** and **12** was much greater than the thermodynamic stability of **13**.

Thus, the selectivity for the self-assembly of the homo or hetero cavitand cage is controlled by the balance between kinetic and thermodynamic stabilities of cages based on a combination of factors such as coordination ability and steric demand of the cavitands. Selective formation of hetero cavitand cages **10** and **13** has been achieved by controlling the addition order of cavitand ligands through dynamic self-assembly based on kinetic control. This work presented here could have implications for constructing dynamic supramolecular structures akin to biological systems.

Experimental Section

General. ^{1}H NMR spectra were recorded at 300 MHz on a Bruker AC300 spectrometer. ^{19}F and ^{31}P NMR spectra were recorded at 376 and 162 MHz, respectively, on a JEOL JNM-AL400 spectrometer. CSI-MS spectra were measured on a JEOL JMS-700 spectrometer. Syntheses of cavitands (**1**, **2**, and **3**) and characterizations of self-assembled cavitand cages (**6**, **8**, and **9**) were described previously.[11]

{1·2a·[Pt(dppp)]$_4$}$^{8+}$·(TfO$^-$)$_8$ (7). ^{1}H NMR ($CDCl_3$) δ 0.88 (t, J = 6.4 Hz, 12H), 0.89 (t, J = 6.7 Hz, 12H), 1.10−1.58 (m, 80H), 2.18−2.50 (m, 24H), 2.95−3.11 (m, 8H), 3.31−3.50 (m, 8H), 4.25 (d, J = 7.6 Hz, 4H), 4.39 (d, J = 6.5 Hz, 4H), 4.69 (t, J = 8.6 Hz, 4H), 4.82 (t, J = 8.6 Hz, 4H), 4.83 (d, J = 7.6 Hz, 4H), 5.76 (d, J = 6.5 Hz, 4H), 6.92 (brs, 8H), 7.03 (d, J = 6.3 Hz, 8H), 7.06 (s, 4H), 7.10 (d, J = 6.9 Hz, 8H), 7.15−7.24 (m, 28H), 7.39−7.52 (m, 28H), 7.52−7.63 (m, 16H), 7.73−7.90 (m, 16H), 8.92 (brs, 8H); ^{19}F NMR ($CDCl_3$) δ −80.07; ^{31}P NMR ($CDCl_3$) δ −16.31 (d, $^2J_{P-P}$ = 31.9 Hz, J_{P-Pt} = 2810 Hz), −15.02 (d, $^2J_{P-P}$ = 31.9 Hz, J_{P-Pt} = 3680 Hz); CSI MS m/z 2948.4 [**7** − 2(TfO$^-$)]$^{2+}$ (calcd 2947.8), 1915.8 [**7** − 3(TfO$^-$)]$^{3+}$ (calcd 1915.5), 1399.2 [**7** − 4(TfO$^-$)]$^{4+}$ (calcd 1399.2).

{2b·3·[Pd(dppp)]$_4$}$^{8+}$·(TfO$^-$)$_8$ (10). ^{1}H NMR ($CDCl_3$) δ 0.89 (t, J = 7.1 Hz, 24H), 1.22−1.51 (m, 112H), 2.15−2.41 (m, 24H), 2.81−3.02 (m, 8H), 3.14−3.28 (m, 8H), 4.51 (d, J = 7.3 Hz, 4H), 4.65 (t, J = 8.4 Hz, 4H), 4.70−4.95 (overlap, 12H), 5.99 (d, J = 7.3 Hz, 4H), 6.62 (m, 8H), 7.06 (d, J = 8.6 Hz, 8H), 7.14 (s, 4H), 7.20 (m, 8H), 7.28−7.76 (m or overlap, 68H), 7.86 (dd, J = 3.3, 8.2 Hz, 16H), 8.85

(m, 8H); ^{19}F NMR ($CDCl_3$) δ −80.03; ^{31}P NMR ($CDCl_3$) δ 5.18 (d, $^2J_{P-P}$ = 27.3 Hz), 11.88 (d, $^2J_{P-P}$ = 27.3 Hz); CSI MS *m*/*z* 2933.0 [**10** − 2(TfO$^-$)]$^{2+}$ (calcd 2930.7), 1905.0 [**10** − 3(TfO$^-$)]$^{3+}$ (calcd 1904.2).

{(2b)$_2$·[Pt(dppp)]$_4$}$^{8+}$·(TfO$^-$)$_8$ (11b). ^{1}H NMR (CD_2Cl_2) δ 0.88 (t, *J* = 6.8 Hz, 24H), 1.20−1.60 (m, 144H), 2.24−2.42 (m, 24H), 2.94−3.10 (m, 16H), 4.21 (d, *J* = 7.2 Hz, 8H), 4.70 (t, *J* = 8.0 Hz, 8H), 5.08 (d, *J* = 7.2 Hz, 8H), 7.00 (d, *J* = 8.6 Hz, 16H), 7.11 (d, *J* = 8.6 Hz, 16H), 7.34 (s, 8H), 7.45−7.60 (m, 48H), 7.74 (dd, *J* = 7.5, 11.8 Hz, 32H); ^{1}H NMR ($CDCl_3$) δ 0.89 (t, *J* = 6.9 Hz, 24H), 1.20−1.55 (m, 144H), 2.17−2.42 (m, 24H), 2.99−3.17 (m, 16H), 4.26 (d, *J* = 6.4 Hz, 8H), 4.70 (t, *J* = 7.7 Hz, 8H), 5.12 (d, *J* = 6.4 Hz, 8H), 7.00−7.15 (m, 24H), 7.27−7.46 (m, 48H), 7.48−7.59 (m, 48H), 7.68−7.84 (m, 32H); ^{19}F NMR (CD_2Cl_2) δ −80.61; ^{31}P NMR (CD_2Cl_2) δ −15.14 (J_{P-Pt} = 3420 Hz); CSI MS *m*/*z* 3219.5 [**11b** − 2(TfO$^-$)]$^{2+}$ (calcd 3220.4).

{(3)$_2$·[Pt(dppp)]$_4$}$^{8+}$·(TfO$^-$)$_8$ (12). ^{1}H NMR (CD_2Cl_2) δ 0.89 (t, *J* = 6.9 Hz, 24H), 1.22−1.49 (m, 80H), 2.11−2.30 (m, 24H), 3.20−3.36 (m, 16H), 4.17 (d, *J* = 7.3 Hz, 8H), 4.74 (t, *J* = 8.0 Hz, 8H), 5.90 (d, *J* = 7.3 Hz, 8H), 7.02 (d, *J* = 6.3 Hz, 16H), 7.03 (s, 8H), 7.38−7.52 (m, 48H), 7.58−7.72 (m, 32H), 8.95 (d, *J* = 6.5 Hz, 16H); ^{1}H NMR ($CDCl_3$) δ 0.89 (t, *J* = 6.9 Hz, 24H), 1.19−1.53 (m, 80H), 2.10−2.38 (m, 24H), 3.24−3.40 (m, 16H), 4.25 (d, *J* = 7.1 Hz, 8H), 4.76 (t, *J* = 8.0 Hz, 8H), 5.93 (d, *J* = 7.1 Hz, 8H), 7.06 (d, *J* = 6.5 Hz, 16H), 7.13 (s, 8H), 7.35−7.57 (m, 48H), 7.57−7.70 (m, 32H), 8.95 (d, *J* = 6.5 Hz, 16H); ^{19}F NMR (CD_2Cl_2) δ −80.65; ^{31}P NMR (CD_2Cl_2) δ −15.11 (J_{P-Pt} = 3060 Hz); CSI MS *m*/*z* 6139.5 (**12** − TfO$^-$)$^+$ (calcd 6141.0), 2994.9 [**12** − 2(TfO$^-$)]$^{2+}$ (calcd 2996.0), 1946.7 [**12** − 3(TfO$^-$)]$^{3+}$ (calcd 1947.6).

{2b·3·[Pt(dppp)]$_4$}$^{8+}$·(TfO$^-$)$_8$ (13). ^{1}H NMR (CD_2Cl_2) δ 0.89 (t, *J* = 6.9 Hz, 12H), 0.91 (t, *J* = 6.6 Hz, 12H), 1.21−1.55 (m, 112H), 2.18−2.50 (m, 24H), 2.87−3.05 (m, 8H), 3.17−3.34 (m, 8H), 4.19 (d, *J* = 7.2 Hz, 4H), 4.38 (d, *J* = 7.3 Hz, 4H), 4.61 (t, *J* = 8.0 Hz, 4H), 4.72 (d, *J* = 7.2 Hz, 4H), 4.82 (t, *J* = 7.6 Hz, 4H), 6.03 (d, *J* = 7.3 Hz, 4H), 6.58 (brs, 8H), 7.07 (d, *J* = 8.7 Hz, 8H), 7.19 (d, *J* = 6.0 Hz, 4H), 7.25 (s, 4H), 7.31 (dt, *J* = 2.7, 7.7 Hz, 4H), 7.36−7.55 (m, 44H), 7.56−7.68 (m, 16H), 7.80−7.93 (m, 16H), 8.83 (d, *J* = 6.0 Hz, 8H); ^{1}H NMR ($CDCl_3$) δ 0.88 (t, *J* = 6.4 Hz, 24H), 1.17−1.57 (m, 112H), 2.12−2.47 (m, 24H), 2.90−3.08 (m, 8H), 3.18−3.43 (m, 8H), 4.31 (d, *J* = 7.2 Hz, 4H), 4.50 (d, *J* = 7.0 Hz, 4H), 4.63 (t, *J* = 7.9 Hz, 4H), 4.81 (d, *J* = 7.2 Hz, 4H), 4.84 (t, *J* = 8.0 Hz, 4H), 6.00 (d, *J* = 7.0 Hz, 4H), 6.60 (m, 8H), 7.06 (d, *J* = 8.7 Hz, 8H), 7.19 (dd, *J* = 6.1, 10.7 Hz, 4H), 7.28−7.34 (m, 16H), 7.34−7.55 (m, 16H), 7.55−7.67 (m, 24H), 7.65−7.94 (m, 16H), 8.89 (s like, 8H); ^{19}F NMR (CD_2Cl_2) δ −80.47; ^{31}P NMR (CD_2Cl_2) δ −17.01 (d, $^2J_{P-P}$ = 31.9 Hz, J_{P-Pt} = 2860 Hz), −12.37 (d, $^2J_{P-P}$ = 31.9 Hz, J_{P-Pt} = 3610 Hz); CSI MS *m*/*z* 6361.0 (**13** − TfO$^-$)$^+$ (calcd 6365.4), 3107.0 [**13** − 2(TfO$^-$)]$^{2+}$ (calcd 3108.2), 2021.4 [**13** − 3(TfO$^-$)]$^{3+}$ (calcd 2022.4).

Acknowledgment. We thank Prof. Takayuki Kawashima and Prof. Kei Goto (The University of Tokyo) for our use of their ^{19}F and ^{31}P NMR spectrometer. This work was supported in part by Grants-in-Aid from the Ministry of Education, Science, Sports, Culture, and Technology of Japan (No. 17350067 to K.K.) and by the Sasakawa Scientific Research Grant from The Japan Science Society (to M.Y.).

JA0555365